Thirteenth USA/Europe Air Traffic Management Research and Development Seminar (ATM2019)

Direct Modeling of Flight Time Uncertainty as a Function of Flight Condition and Weather Forecast

Noboru Takeichi and Taiki Yamada
Department of Aeronautics and Astronautics
Tokyo Metropolitan University
Hino, Tokyo, JAPAN
takeichi@tmu.ac.jp

Abstract— **This study presents a direct prediction model of flight time uncertainty as a function of flight condition and weather forecast information at an arbitrary flight distance. Due to fluctuations in meteorological conditions, flight time uncertainty increase is unavoidable despite constant monitoring and control of the aircraft's Mach number, flight altitude, and direction. Using secondary surveillance radar Mode S and numerical weather forecast, actual flight data are collected and processed in order to obtain a large dataset regarding flight time error and flight and meteorological conditions. The law of propagation of uncertainty is utilized to derive a mathematical model of flight time uncertainty as a function of ground speed, Mach number, flight distance, wind, temperature, and pressure altitude. Through cluster and linear regression analyses, the coefficients of the derived function are determined, taking into consideration the correlation between temperature and pressure altitude. Upon evaluation, the proposed model function is found to directly predict flight time uncertainty, without underestimation or overestimation even under moderate or severe weather conditions, at an arbitrary distance. The results show that the direct prediction model simultaneously improves the safety and efficiency of 4D trajectory management.**

Keywords-air traffic management; 4D trajectory management; flight time uncertainty; modeling and validation

I. INTRODUCTION

Civil aviation authorities plan to introduce a time-based operation to future air traffic management systems [1–3] as a long-term strategy in dealing with the increasing air transportation demand. An accurate and reliable flight time prediction is believed to improve the safety and efficiency of air traffic management [4]. The application of this concept has been investigated in certain studies, such as displaying arrival time uncertainty on the monitors of air traffic controllers (ATCs) and pilots [5–7] and determination of the freeze horizon of an arrival manager [8]. Operational time uncertainty is correlated to with certain factors, such as departure time uncertainty; weather prediction errors; tracking, navigation, and control errors; and tactical aircraft control errors. This study focuses on flight time uncertainty caused by weather uncertainty and aircraft control errors to contribute airborne and ground-based 4D trajectory management, such as arrival time control and time-based separation at runway thresholds and merging points, etc.

Previous studies considered flight time uncertainty modeling as a part of trajectory uncertainty for conflict prediction, which regarded the standard deviation of aircraft positioning error as an evaluation index. Such studies theoretically proved the linear proportionality of standard deviation relative to flight distance or time [4, 9], as validated by empirical data analyses of position uncertainty [10–12]. Additionally, a "dynamic spacing" concept was implied [13] where position uncertainty is associated with meteorological conditions for safer and more efficient management of air traffic. This concept aside, static modeling of trajectory uncertainty had been widely applied in researches in air traffic management [14–17]. With respect to trajectory uncertainty prediction based on meteorological conditions, modeling of wind uncertainty correlation between aircraft pairs [18, 19] and its application for conflict resolution [20] was considered. Specifically, wind uncertainty estimates based on ensemble weather prediction data were used for prediction of trajectory [21, 22] and fuel consumption [23] uncertainties. Recently, flight time uncertainty was found to be related to temporal crosswind and temperature, as well as the tailwind, both in ground-based and airborne 4D trajectory predictions [24, 25]. A fluctuation model of the ground speed (GS) as a function of true airspeed (TAS), Mach number, wind, and temperature [26] was also developed. The GS fluctuation model demonstrated correct estimation of flight time uncertainty under arbitrary meteorological conditions; nevertheless, it was unable to provide an accurate prediction of increase of flight time uncertainty in accordance with flight distance [27].

An aircraft usually maintains its pressure altitude constant during cruise flights; nevertheless, its geodetic altitude is not necessarily constant due to fluctuations of pressure altitude. Thus, it is presumed that fluctuations of geodetic altitude results in a fluctuation of GS due to the exchange between the potential and kinetic energies. As this is also a cause of the flight time uncertainty, the application of pressure altitude information is expected to improve the accuracy of the flight time uncertainty prediction.

In this study, it is aimed to develop a model of the flight time uncertainty as a function of flight conditions and numerical weather forecast data. Specifically, in order to improve the authors' previous prediction model [26], the pressure altitude information in the weather forecast is additionally introduced for modeling. In addition, the previous model estimated the GS fluctuation by using flight condition and weather forecast [26] to indirectly predict the flight time uncertainty, which is considered the reason of incapability of correct prediction at an

arbitrary distance. Hence it is further aimed to develop a model function capable of direct prediction of the flight time uncertainty to enable the prediction of the flight time uncertainty at an arbitrary flight distance. In the 4D trajectory management concept [28], it is supposed that the estimated time of arrival is computed on-board and sent to ground systems and ATCs. This procedure is simulated herein, through estimation of flight time error following the same algorithms as the onboard computation. Initially, a model function of flight time uncertainty is derived mathematically using the law of uncertainty propagation. Subsequently, the coefficients of the derived function are analyzed through cluster and regression analyses via actual operational and numerical weather forecast data. Finally, the model's effectiveness is evaluated.

II. DATA FOR ANALYSIS

Flight data collected by the SSR Mode S placed in Tokyo and Sendai in Japan in March, June, September and December in 2015 and 2016 are applied in this study. These data include the aircraft type, IAS, true airspeed (TAS), GS, Mach number, pressure altitude, azimuth angle, and true track angle recorded every 10s [29]. For the weather forecast data, the Global Spectral Model (GSM) of the numerical forecast data [30] are applied. The GSM data are updated every 6 hours and provides the temperature and wind forecast information every 3 hours for next 84 hours at grid points placed every 0.25 degrees in longitude and 0.2 degrees in latitude at every 50-100 hPa pressure altitudes. In the analysis, the forecast values are calculated using linear interpolation on time, longitude, latitude and pressure altitude using newest forecast data. Cruising aircraft are usually controlled to maintain the Mach number, track angle and pressure altitude. Therefore, the flight trajectories continuously satisfying the following conditions for more than 100 km are extracted, and regarded as controlled ones: pressure altitude above 25000 ft, true track angle between 30-150 degrees, maintaining Mach number within 0.02, true track angle within 5deg and pressure altitude within 100ft. Finally, 62713 trajectories shown in Fig. 1 are extracted.

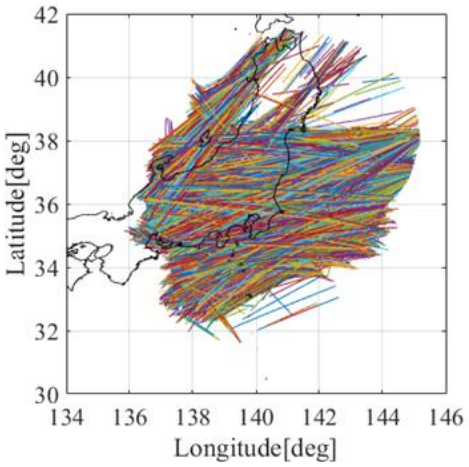

Figure 1. Extracted Trajectories (N=62713)

III. DIRECT MODELING OF FLIGHT TIME UNCERTAINTY

A. Flight Time Error Calculation

The flight time error is defined as the time difference between the predicted flight time and actual time. Predicted flight time t_{pred} is calculated on board using initial GS $V_{GS,ini}$ measured by INS and GPS at the moment of prediction as (1) where D is the flight distance. Actual flight time t_{act} is calculated through the time integration of the recoded actual GS $V_{GS,act}$ as (2). Flight time error t_{err} is defined as their difference as described in (3).

$$t_{pred} = \frac{D}{V_{GS,ini}} \tag{1}$$

$$\int_0^{t_{act}} V_{GS,act}\,dt = D \tag{2}$$

$$t_{err} \triangleq t_{act} - t_{pred} \tag{3}$$

This calculation corresponds to the assumptions that the GS data in the SSR Mode S are correct, and that there are no differences in any flight time error mechanisms among aircraft types. The time-histories of the flight time error of the extracted trajectories are shown in Fig. 2, and the distribution of the flight time error at 100 km interval in the 100–500 km range is summarized in Fig. 3. The increase behavior of the flight time uncertainty with the flight distance is shown in Fig. 4, which reveal that its increase is apparently larger than the linear increase as indicated in [27]. The histograms of the flight time, flight distance [km], and initial values of Mach number, GS [m/s], tailwind speed [m/s], absolute value of crosswind speed [m/s], temperature [K], and altitude [ft] are summarized in Fig. 5. The flight times of the sample trajectories shown in Fig. 5a are so short compared with the weather forecast time horizon of the GSM model and its update frequency that it is assumed that the temporal deterioration of weather forecast accuracy is negligible. For example, the mean and standard deviations and RMS of the flight time error are -0.19s, 7.24s and 7.24s, respectively, at the distance of 200 km. These show that the flight time error follows almost zero-mean and mound-shaped distributions. As actual trajectory and weather forecast data are analyzed in this study, the mean square and RMS, instead of variance and standard deviation (STD), are evaluated as the measure of flight time uncertainty in actual data analyses.

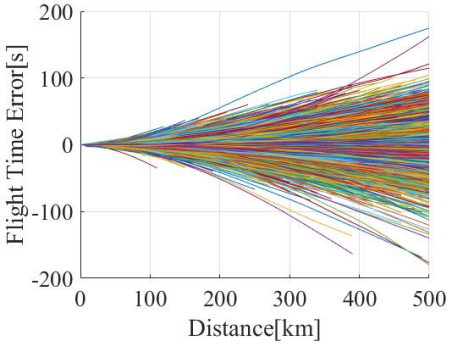

Figure 2. Histories of Flight Time Error (N=62713)

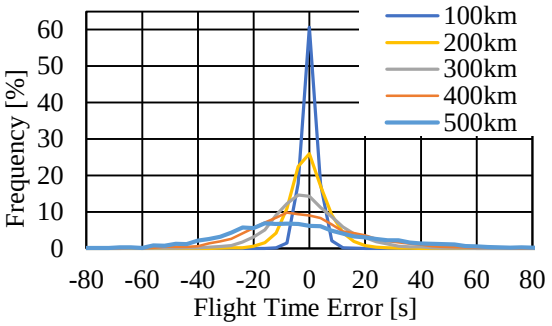

Figure 3. Distribution of Flight Time Error at 100~500km

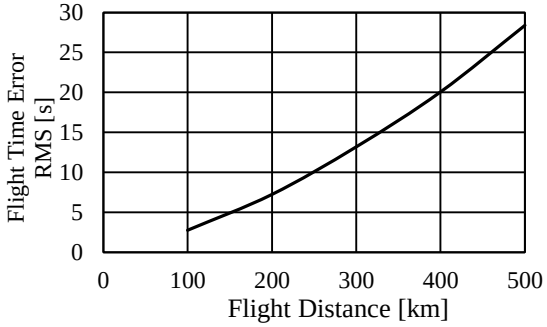

Figure 4. Increase of flight Time Uncertainty

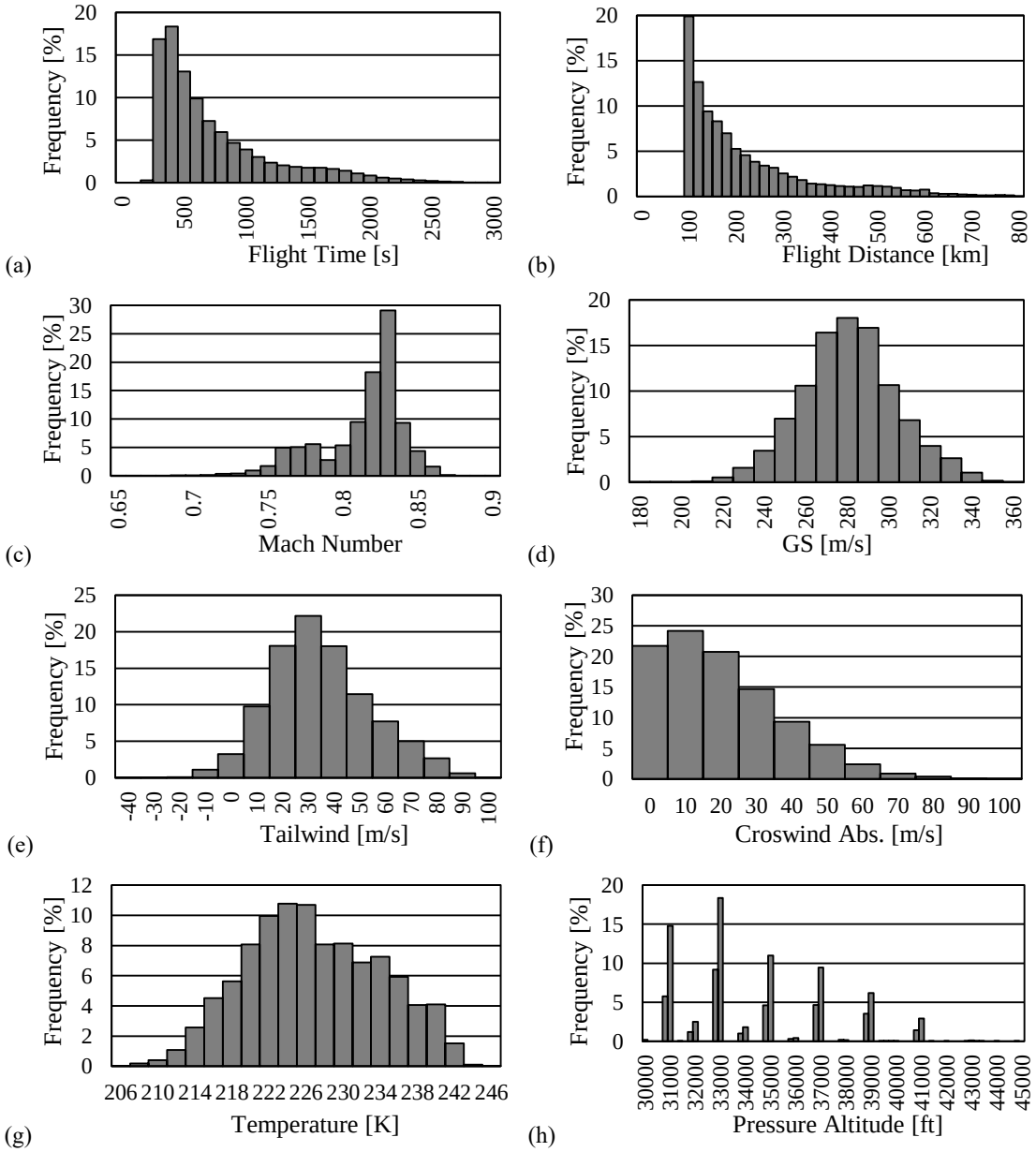

Figure 5. Histograms, a: Flight Time, b: Flight Distance, and Initial Values of c: Mach number, d: GS, e: Tailwind Speed, f: Absolute Value of Crosswind Speed, g: Air Temperature, h: Pressure Altitude (N=62713)

B. Theoretical Basis

The mathematical expression of the flight time t_f predicted onboard is:

$$t_f = \frac{D}{V_{GS}} \tag{4}$$

where V_{GS} is the GS measured at the moment of prediction. The GS variance σ_{GS}^2 was considered static in the past studies [4,9,10,13]. In this regard, the variance of the flight time $\sigma_{t_f}^2$ is obtained through the total differential of (4) as follows:

$$\sigma_{t_f}^2 = \left(\frac{D}{V_{GS}^2}\right)^2 \sigma_{GS}^2 \tag{5}$$

which indicates that the flight time variance is inversely proportional to the quartic power of the GS, square proportional to the flight distance, and linear proportional to GS variance σ_{GS}^2. In the authors' previous study [26,27], the GS variance was modeled using the real gas constant for air $R = 287.1\left[m^2/Ks^2\right]$ and the Adiabatic index for air $\kappa = 1.4$ as follows:

$$\sigma_{GS}^2 = \left(1+\left(\frac{W_c}{V_{TAStr}}\right)^2\right)\sigma_W^2 + \left(\frac{M^2\kappa R}{2V_{TAStr}}\right)^2 \sigma_T^2 + \left(\frac{M\kappa RT}{V_{TAStr}}\right)^2 \sigma_M^2 \tag{6}$$

, where W_c, V_{TAStr}, M and T denote crosswind speed, along track TAS, Mach number and temperature, respectively. Nevertheless, this model failed to capture the nonlinear increase of the flight time uncertainty depicted in Fig. 4 [27]. Dealing with the nonlinear behavior requires the model function to directly treat flight time uncertainty $\sigma_{t_f}^2$ as a function of flight and meteorological conditions.

As the GS is a function of wind, temperature, pressure altitude and Mach number, t_f could be described as follows:

$$t_f = f\left(D, M, W_t, W_c, T, h\right) \tag{7}$$

where h is geodetic altitude. From this expression, the total differential with independent variables tailwind W_t, W_c, M, T and h is obtained as:

$$dt_f = \frac{\partial f}{\partial M}dM + \frac{\partial f}{\partial W_t}dW_t + \frac{\partial f}{\partial W_c}dW_c + \frac{\partial f}{\partial T}dT + \frac{\partial f}{\partial h}dh \tag{8}$$

The partial derivative terms for dM, dW_t, dW_c, dT are derived from the following equations:

$$V_{GS} = V_{TAStr} + W_t \tag{9}$$

and

$$V_{TAStr} = \sqrt{V_{TASm} - W_c^2} = \sqrt{M^2\kappa RT - W_c^2} \tag{10}$$

which describe the translation of the Mach number measured onboard into the GS based on the geometry of velocity vectors shown in Fig. 6, and V_{TASm} refers to TAS measured onboard. Applying partial differentiation to these equations gives:

$$\begin{aligned}\frac{\partial f}{\partial M} &= -\frac{D}{\left(\sqrt{M^2\kappa RT - W_c^2} + W_t\right)^2}\cdot\frac{M\kappa RT}{\sqrt{M^2\kappa RT - W_c^2}} \\ &= -\frac{D}{V_{GS}^2}\cdot\frac{M\kappa RT}{V_{TAStr}}\end{aligned} \tag{11}$$

$$\frac{\partial f}{\partial W_t} = \frac{D}{\left(\sqrt{M^2\kappa RT - W_c^2} + W_t\right)^2} = -\frac{D}{V_{GS}^2} \tag{12}$$

$$\begin{aligned}\frac{\partial f}{\partial W_c} &= \frac{D}{\left(\sqrt{M^2\kappa RT - W_c^2} + W_t\right)^2}\cdot\frac{W_c}{\sqrt{M^2\kappa RT - W_c^2}} \\ &= \frac{D}{V_{GS}^2}\cdot\frac{W_c}{V_{TAStr}}\end{aligned} \tag{13}$$

$$\begin{aligned}\frac{\partial f}{\partial T} &= -\frac{D}{\left(\sqrt{M^2\kappa RT - W_c^2} + W_t\right)^2}\cdot\frac{M^2\kappa R}{2\sqrt{M^2\kappa RT - W_c^2}} \\ &= -\frac{D}{V_{GS}^2}\cdot\frac{M^2\kappa R}{2V_{TAStr}}\end{aligned} \tag{14}$$

The partial derivative term for dh is obtained from the law of conservation of mechanical energy:

$$\frac{1}{2}V_{GS}^2 + gh = const. \tag{15}$$

wherein the total differential yields:

$$dV_{GS} = -\frac{g}{V_{GS}}dh \tag{16}$$

From the above equation and the total differential of (4), the differential for t_f becomes:

$$dt_f = -\frac{D}{V_{GS}^2}dV_{GS} = \frac{Dg}{V_{GS}^3}dh \tag{17}$$

Finally, the total differential (8) is expressed as:

$$\begin{aligned}dt_f = &-\frac{D}{V_{GS}^2}dW_t + \frac{D}{V_{GS}^2}\frac{W_c}{V_{TAStr}}dW_c \\ &-\frac{D}{V_{GS}^2}\frac{M^2\kappa R}{2V_{TAStr}}dT - \frac{D}{V_{GS}^2}\frac{M\kappa RT}{V_{TAStr}}dM + \frac{Dg}{V_{GS}^3}dh\end{aligned} \tag{18}$$

Applying the law of propagation of uncertainty [31], the variance of the flight time prediction error $\sigma_{t_f}^2$ is obtained as:

$$\sigma_{t_f}^2 = \left(\frac{D}{V_{GS}^2}\right)^2\left(1+\left(\frac{W_c}{V_{TAStr}}\right)^2\right)\sigma_W^2 + \left(\frac{D}{V_{GS}^2}\right)^2\left(\frac{M^2\kappa R}{2V_{TAStr}}\right)^2\sigma_T^2 + \left(\frac{D}{V_{GS}^2}\right)^2\left(\frac{M\kappa RT}{V_{TAStr}}\right)^2\sigma_M^2 + \left(\frac{D}{V_{GS}^2}\right)^2\left(\frac{g}{V_{GS}}\right)^2\sigma_h^2 - \frac{D^2}{V_{GS}^5}\frac{M^2\kappa R}{V_{TAStr}}g\sigma_{Th} \quad (19)$$

, where no correlation is assumed for all variables, except for T and h, which are presumed to exhibit a strong correlation. Moreover, wind fluctuation is assumed to be homogeneous in all directions.

Meteorological conditions under which an aircraft operates behave in the same manner as forecast conditions to be used in the model function, with expected differences in their magnitudes as numerical weather forecast generally provides discrete data, whereas the actual meteorological condition is continuous. Hence the coefficient α is introduced in this study in order to compensate for such difference. Additionally, being unavailable at the moment of prediction, σ_M^2 is treated as a constant value as α_3. With these considerations, x is introduced to the model function as a descriptor of explanatory variables:

$$\begin{aligned}\sigma_{t_f}^2 &= \alpha_1\left(\frac{D}{V_{GS}^2}\right)^2\left(1+\left(\frac{W_c}{V_{TAStr}}\right)^2\right)\sigma_W^2 + \alpha_2\left(\frac{D}{V_{GS}^2}\right)^2\left(\frac{M^2\kappa R}{2V_{TAStr}}\right)^2\sigma_T^2 \\ &+\alpha_3\left(\frac{D}{V_{GS}^2}\right)^2\left(\frac{M\kappa RT}{V_{TAStr}}\right)^2 + \alpha_4\left(\frac{D}{V_{GS}^2}\right)^2\left(\frac{g}{V_{GS}}\right)^2\sigma_h^2 \\ &-\alpha_5\frac{D^2}{V_{GS}^5}\frac{M^2\kappa R}{V_{TAStr}}g\sigma_{Th} \\ &= \alpha_1 x_1 + \alpha_2 x_2 + \alpha_3 x_3 + \alpha_4 x_4 + \alpha_5 x_5\end{aligned} \quad (20)$$

where the x parameters are defined as:

$$\begin{aligned}&x_1 \triangleq \left(\frac{D}{V_{GS}^2}\right)^2\left(1+\left(\frac{W_c}{V_{TAStr}}\right)^2\right)\sigma_W^2,\ x_2 \triangleq \left(\frac{D}{V_{GS}^2}\right)^2\left(\frac{M^2\kappa R}{2V_{TAStr}}\right)^2\sigma_T^2, \\ &x_3 \triangleq \left(\frac{D}{V_{GS}^2}\right)^2\left(\frac{M\kappa RT}{V_{TAStr}}\right)^2,\ x_4 \triangleq \left(\frac{D}{V_{GS}^2}\right)^2\left(\frac{g}{V_{GS}}\right)^2\sigma_h^2, \\ &x_5 \triangleq -\frac{D^2}{V_{GS}^5}\frac{M^2\kappa R}{V_{TAStr}}g\sigma_{Th}\end{aligned} \quad (21)$$

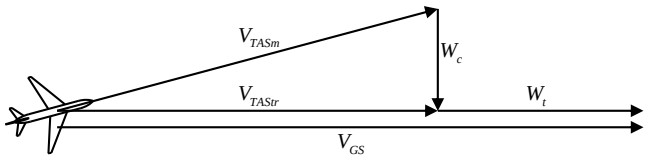

Figure 6. Geometry of Aircraft GS, TAS and Wind Speed

C. Modeling: Cluster Analysis and Regression

Cluster and regression analyses were employed to appropriately determine the coefficients in (20). The cluster analysis [32] is applied for construction data groups having similar trajectories, prior to the collection of RMS values of flight time errors and average of the initial values of x parameters, which are determined using the initial values of GS, Mach number, tailwind, crosswind, temperature and geodetic altitude and their variances. This procedure corresponds to the prediction of flight time uncertainty of a trajectory using the Mach number at the moment of the prediction and the meteorological conditions to which the aircraft is subjected. Afterward, multiple linear regression using the cluster data is performed to determine the coefficients of the prediction model function.

Half of the trajectory data are applied for cluster and regression analyses, whereas the rest are prepared for validation, which will be discussed in the next section. For the model function to be capable of uncertainty prediction at an arbitrary flight distance, $x_{1,ini} \sim x_{5,ini}$ are selected as the feature parameters of clustering to cover all parameters affecting flight time uncertainty. The dataset for the cluster analysis consisted of 31356 vectors defined as follows:

$$\mathbf{y}_i \triangleq \left(x_{1,ini}, x_{2,ini}, x_{3,ini}, x_{4,ini}, x_{5,ini}\right)^T \quad (22)$$

where

$$\begin{aligned}&x_{1,ini} \triangleq \left(\frac{D}{V_{GS,ini}^2}\right)^2\left(1+\left(\frac{W_{c,ini}}{V_{TAStr,ini}}\right)^2\right)\sigma_W^2, \\ &x_{2,ini} \triangleq \left(\frac{D}{V_{GS,ini}^2}\right)^2\left(\frac{M_{ini}^2\kappa R}{2V_{TAStr,ini}}\right)^2\sigma_T^2, \\ &x_{3,ini} \triangleq \left(\frac{D}{V_{GS,ini}^2}\right)^2\left(\frac{M_{ini}\kappa RT_{ini}}{V_{TAStr,ini}}\right)^2, \\ &x_{4,ini} \triangleq \left(\frac{D}{V_{GS,ini}^2}\right)^2\left(\frac{g}{V_{GS,ini}}\right)^2\sigma_h^2, \\ &x_{5,ini} \triangleq -\frac{D^2}{V_{GS,ini}^5}\frac{M_{ini}^2\kappa R}{V_{TAStr,ini}}g\sigma_{Th}\end{aligned} \quad (23)$$

where the subscript ini indicates that the values are obtained at the moment of prediction. The variances and covariance of weather forecast data are calculated using these equations:

$$\sigma_W^2 = \frac{1}{N}\sum_{i=1}^{N}\left\|\mathbf{W}_i - \mathbf{W}_{ini}\right\|^2 \quad (24)$$

$$\sigma_T^2 = \frac{1}{N}\sum_{i=1}^{N}\left(T_i - T_{ini}\right)^2 \quad (25)$$

$$\sigma_h^2 = \frac{1}{N}\sum_{i=1}^{N}\left(h_i - h_{ini}\right)^2 \tag{26}$$

$$\sigma_{Th} = \frac{1}{N}\sum_{i=1}^{N}\left(T_i - T_{ini}\right)\left(h_i - h_{ini}\right) \tag{27}$$

where $\mathbf{W} \triangleq \left(W_t, W_c\right)^T$. $\mathbf{W}_i$, T_i, h_i and $\mathbf{W}_{ini}$, T_{ini} and h_{ini} are the i th and initial components of each trajectory data, respectively.

The Gaussian mixture model using the Expectation–maximization algorithm (GMM-EM) [32], a type of soft clustering, is applied for the cluster analysis. It creates clusters to achieve near-Gaussian distribution of each parameter, which is suitable for the analysis of statistical values. To obtain as appropriate statistical parameters as possible, a sample vector with a posterior probability below that corresponding to the range four times the STD value in each cluster is judged as an anomaly and is thereby excluded from the cluster. Additionally, if the number of sample vectors in a cluster is below 50, then that cluster gets eliminated from the regression analysis. Sensitivity analysis on the Bayesian information criterion (BIC) [31] is conducted to determine the appropriate number of clusters, where the BIC average values were obtained from the repetition of the cluster analysis, thirty times for each number of clusters. As the BIC rewards accuracy, and penalizes the number of clusters, the minimum BIC value indicates the appropriate number of clusters that achieve adequate accuracy. From the result shown in Fig. 7, the appropriate number of clusters to minimize the BIC value is obtained as 120.

The actual flight time error variance $\sigma_{t_f}^2$ of each data cluster is calculated as mean square as:

$$\sigma_{t_f,act}^2 = mean\left(t_{err}^2\right) \tag{28}$$

The mean values of $x_{1,ini} \sim x_{5,ini}$ are also obtained for each cluster, denoted as $x_{1,c} \sim x_{5,c}$, respectively. Using these parameters, the direct prediction model function is expressed as:

$$\sigma_{t_f,act}^2 = \alpha_1 x_{1,c} + \alpha_2 x_{2,c} + \alpha_3 x_{3,c} + \alpha_4 x_{4,c} + \alpha_5 x_{5,c} \tag{29}$$

Finally, in order to determine the coefficient $\alpha_1 \sim \alpha_5$ multiple linear regression is applied.

From the GMM-EM analysis, fifty-eight clusters are obtained. The correlation between $\sigma_{t_f,act}^2$ and parameters $x_{1,c} \sim x_{5,c}$ is shown in Fig. 8, and their correlation parameters are summarized in Table I. As all parameters are clarified significant, the regression function of the estimated flight time uncertainty $\sigma_{t_f,est}^2$ is defined as:

$$\sigma_{t_f,est}^2 = 0.28x_1 + 11.40x_2 + 5.6\times10^{-5}x_3 + 0.40x_4 - 12.7x_5 \tag{30}$$

The regression performance is summarized in Table II, which shows the sufficiently large coefficient of determination and T-values for all parameters and sufficiently small p-values, assuring the statistical significance of the regression result. The relationship between the predicted and actual $\sigma_{t_f}^2$ is shown in Fig. 9, which confirms the validity of the regression.

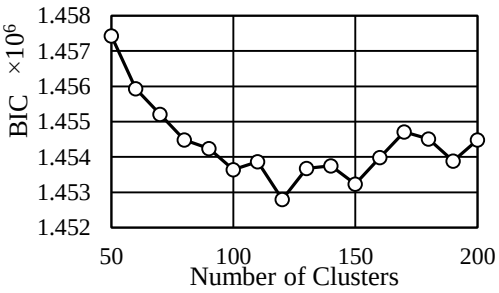

Figure 7. BIC Sensitivity Analysis of Number of Clusters

TABLE I. CORRELATION BETWEEN $x_1 \sim x_5$ AND $\sigma_{t_f,act}^2$

Parameter	Correlation Coefficient	P Value
x_1	0.98	< 0.01
x_2	0.76	< 0.01
x_3	0.96	< 0.01
x_4	0.82	< 0.01
x_5	0.61	< 0.01

TABLE II. SUMMARY OF MULTIPLE LINEAR REGRESSION USING $x_1 \sim x_5$, A: TOTAL, B: PARAMETER

(a)

	Error RMS [s]	Adjusted R^2	P Value
Total	19.3	1.00	< 0.01

(b)

Parameter	Standard Error [s]	T Value	P Value
x_1	1.12×10^{-2}	24.5	< 0.01
x_2	6.16×10^{-1}	18.5	< 0.01
x_3	4.94×10^{-6}	11.3	< 0.01
x_4	11.4×10^{-2}	3.55	< 0.01
x_5	1.05×10^{0}	-12.1	< 0.01

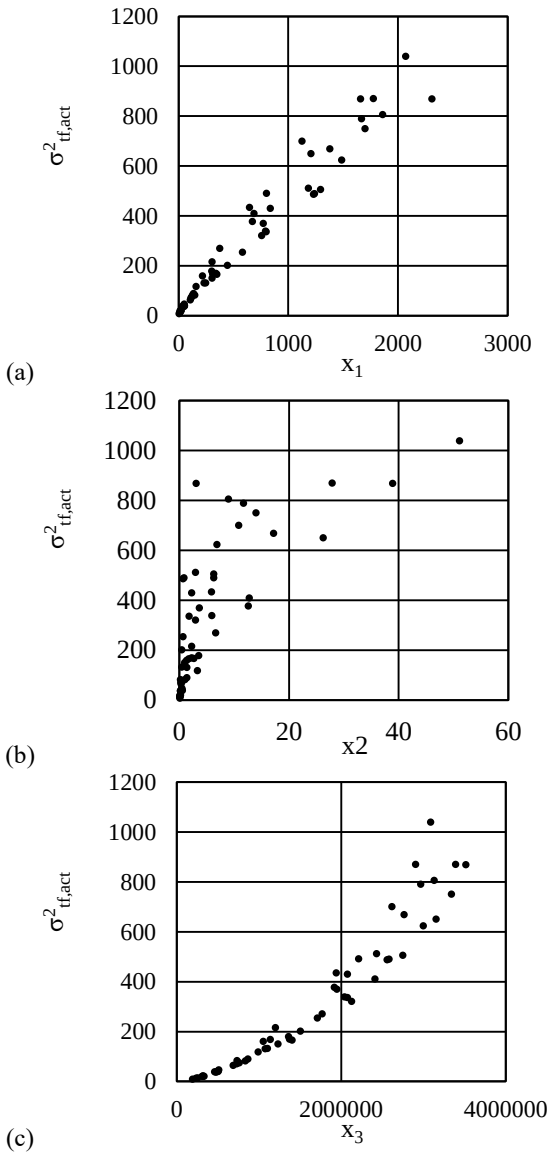

Figure 8. Correlation between $\sigma^2_{t_f,est}$ and Parameters $x_1 \sim x_5$ (N=58), a: x_1 - $\sigma^2_{t_f,est}$ (R=0.98, p<0.01), b: x_2 - $\sigma^2_{t_f,est}$ (R=0.76, p<0.01), c: x_3 - $\sigma^2_{t_f,est}$ (R=-0.96, p=0.19), d: x_4 - $\sigma^2_{t_f,est}$ (R=-0.82, p<0.01), e: x_5 - $\sigma^2_{t_f,est}$ (R=-0.61, p<0.01)

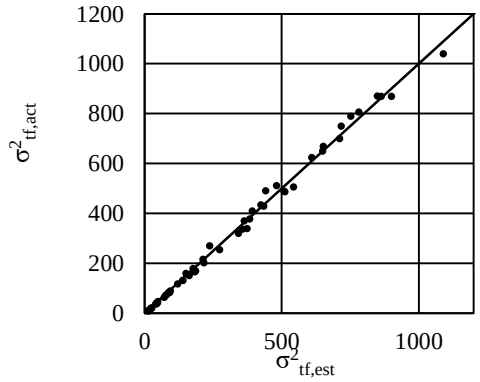

Figure 9. Regression between Estimated and Actual $\sigma^2_{t_f}$ (N=58, R=1.00, p<0.01)

IV. Validation of Direct Prediction Model

The direct prediction model is expected to achieve safe and efficient 4D trajectory management, in accordance with meteorological conditions, as implied in [13], at arbitrary flight distances. If flight time uncertainty becomes larger than average, it will be impossible for a conventional static prediction model to estimate the occurrence of large deviations, leading to loss of safety. By contrast, when flight time uncertainty is smaller than average, a conventional prediction model predicts larger deviations than the actual values. In this case, a larger time-based separation will be necessary, which, in turn, degrades operational efficiency. Therefore, the effectiveness of the direct prediction model is evaluated taking into consideration both larger and smaller $\sigma_{t_f,est}$ cases, which correspond to severe and calm weather conditions, respectively, in comparison with the conventional prediction model at several specific flight distances.

First, the static factor $\sigma^2_{GS,st}$ of the conventional prediction model given in (5) is derived. It is calculated using (31) with the 31356 trajectory data for the regression analysis, obtained as 8.62 [m^2/s^2]:

$$\sigma^2_{GS,st} = mean\left(\frac{V^4_{GS}}{D^2} t^2_{err}\right) \tag{31}$$

Next, using both conventional and direct prediction models, the estimated values of the RMS every 100 km between 100 km and 500 km are obtained for 31356 trajectories for validation. The $\sigma^2_{t_f,act}$, RMS values of the predicted uncertainty of both models every 100km are shown in Fig. 10; it is confirmed that the direct prediction model is able to predict the nonlinear increase behavior of the flight time uncertainty. This result shows the overall validity of the direct prediction model. It is also found that the conventional static prediction model is able to predict the flight time uncertainty correctly around the distance between 100km and 200km because a large number of trajectory samples are available around this range.

To investigate its advantage in detail, the normalized flight time errors are evaluated through division of flight time error with the estimated RMS values. Subsequently, trajectories with both the largest and smallest 25% of $\sigma^2_{t_f,est}$ at every 100 km are particularly utilized to evaluate the effectiveness of the direct prediction model in severe and calm conditions. RMS values are summarized in Table III and Fig.11. According to the result shown in Fig. 10, the prediction accuracy of the direct and conventional predictions are almost same at the distance of 200km. However, the RMS values of the normalized flight time error using the conventional prediction model of the largest and smallest 25% of samples become approximately 1.3 times larger and smaller than 1.0, respectively, as indicated in Table III, whereas the RMS values using the direct prediction model become close to 1.0 in both cases. The difference in RMS values can also be found in the distributions of the normalized flight time error by direct and conventional predictions of the largest and smallest 25% of $\sigma^2_{t_f,est}$ trajectories at the distance of 200km depicted in Fig. 12.

These results clearly demonstrated that the direct prediction model is able to estimate the nonlinear increase behavior of the flight time error, and also capable of its accurate estimation in severe and calm weather conditions without overestimation or underestimation at arbitrary flight distances. In contrast, the conventional prediction model inevitably overestimates and underestimates the flight time error in unusual weather conditions, even when it is able to estimate the overall uncertainty correctly.

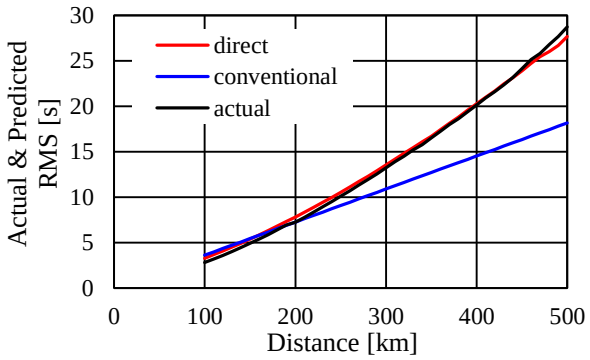

Figure 10. Flight time error rms, black: actual flight time error, red: predicted flight time uncertainty using direct prediction, blue: predicted flight time uncertainty using conventional prediction

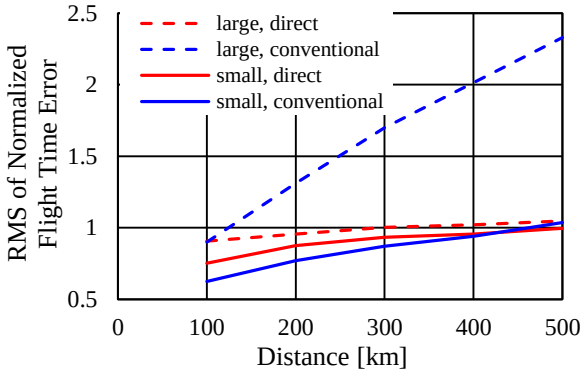

Figure 11. RMS values of normalized flight time error, red: estimated RMS using direct prediction, blue: estimated RMS using conventional prediction, solid: smaller 25% cases, dashed: larger 25% cases

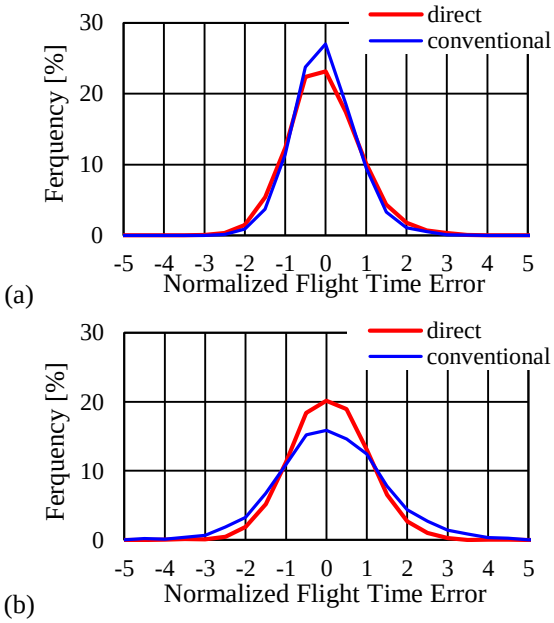

Figure 12. Distributions of normalized flight time uncertainty at 200km, a: Smaller 25% Cases, b: Larger 25% Cases (N=3365)

TABLE III. EVALUATION OF NORMALIZED ERROR

		100km	*200km*	*300km*	*400km*	*500km*
Large $\sigma_{GS,est}$ Group	***Direct Prediction***	0.91	0.96	1.00	1.02	1.05
	Conventional Prediction	0.90	1.31	1.70	2.02	2.33
Small $\sigma_{GS,est}$ Group	***Direct Prediction***	0.75	0.88	0.93	0.96	1.00
	Conventional Prediction	0.62	0.77	0.87	0.94	1.04

V. CONCLUSION

The law of uncertainty propagation was employed to derive a direct prediction model of flight time uncertainty, as a function of flight and meteorological conditions, such as distance, Mach number, wind, temperature, and pressure altitude. For the model function to be capable of accurate prediction of the model function at arbitrary flight distances, all parameters affecting the increase of flight time uncertainty were applied in the cluster and regression analyses. The coefficients of the function were determined through the analyses using actual operational and weather forecast data. After validation, the proposed direct prediction was found to be capable of effectively evaluating flight time uncertainty at arbitrary flight distances, whereas the conventional prediction produced inevitable overestimation or underestimation.

The overestimation of the flight time uncertainty by the conventional static prediction occurs in calm weather conditions. In this case, in a time-based interval management operation, the ATCs would control the time interval between aircraft pairs larger than actually necessary for safety, which can be understood as a potential loss of efficiency. In contrast, the underestimation by the conventional prediction occurs in severe weather conditions. In this case, the ATCs would control the time interval between aircraft pairs smaller than that actually necessary for safety, which can be understood as a potential loss of safety. It is demonstrated that direct prediction evaluates the flight time uncertainty appropriately even in calm or severe weather conditions. Therefore, direct prediction is able to facilitate both safe and efficient 4D trajectory management.

The direct prediction model facilitates the management of flight time uncertainty, which is deemed advantageous when applying 4D trajectory management to air traffic management systems, e.g., ground-based arrival time management and flight speed control for correction, airborne robust speed control for accurate arrival time control, etc. A practical application of flight time uncertainty management, along with new prediction models for ascent and descent trajectories, will be considered in future works. As weather forecast information is readily available in the present air traffic systems, the proposed prediction method is further expected to allow ATCs to manage flight time uncertainty conveniently with enhanced accuracy. With this vision, the management of flight time uncertainly promises smoother air traffic operations within future automated frameworks.

REFERENCES

[1] NextGen Joint Planning and Development Office, "Concept of Operations for the Next Generation Air Transportation System, Version 3.2," Washington, D.C., 2011.

[2] SESAR Joint Undertaking, "Roadmap for Sustainable Air Traffic Management, European ATM Master Plan, edition 2," October 2012.

[3] Japan Civil Aviation Bureau, "Long-term Vision for the Future Air Traffic Systems," 2010.

[4] R.A. Paielli and H. Erzberger, "Conflict Probability Estimation for Free Flight," Journal of Guidance, Control, and Dynamics, Vol. 20, No. 3, 1997, pp. 588-596.

[5] D.B. Nicholls, P. Battino, P. Marti and S. Pozzi, "Presenting Uncertainty to Controllers and Pilots," Proceedings of the 5th USA/Europe Air Traffic Management Research and Development Seminar, Budapest, Jun. 23-27, 2003.

[6] D. Schaefer, A. Gizdavu, and D.B. Nicholls, "The Display of Uncertainty Information on the Working Position," 23rd IEEE/AIAA Digital Avionics Systems Conference, Washington D.C., Oct. 2004.

[7] M. Tielrooij, C. Borst, D. Nieuwenhuisen, M. Mulder and D. Schaefer, "Supporting Arrival Management Decisions by Visualising Uncertainty," Proceedings of the SESAR Innovation Days, Stockholm, Sweden, 2013.

[8] M. Tielrooij, C. Borst, M.M. Van Paassen and M. Mulder, "Predicting Arrival Time Uncertainty from Actual Flight Information," Proceedings of the 11th USA/Europe Air Traffic Management Research and Development Seminar, Lisbon, Jun. 23-26, 2015.

[9] R. Irvine, "a Geometrical Approach to Conflict Probability Estimation," Air Traffic Control Quarterly, Vol. 10, No. 2, 2002, pp. 85-113.

[10] R.A. Paielli, "Empirical Test of Conflict Probability Estimation," USA/Europe Air Traffic Management Rsearch and Development Seminar, Orlando, Dec. 1-4, 1998.

[11] E. Robert and D. De Smedt, "Comparison of Operational Wind Forecasts with Recorded Flight Data," 10th USA/Europe Air Traffic Management Research and Development Seminar, Chicago, June 10-13, 2013.

[12] T.L. Gaydos, W. Kirkman, W. Shresta, E. Blair and J. Kuchenbrod, "Measured Variability and Uncertainty in Flight Operations," IEEE Integrated Communications, Navigation and Surveillance Conference, Herndon, VA, Apr. 24-26, 2012.

[13] G.J. Bakker, H.J. Kremer and H.A.P. Blom, "Geometric and Probabilistic Approaches Towards Conflict Prediction," 3rd USA/Europe Air Traffic Management Rsearch and Development Seminar, Napoli, Jun. 13-16, 2000.

[14] G. Chaloulos, E. Crück and J. Lygeros, "A Simulation Based Study of Subliminal Control for Air Traffic Management," Transpotation Research Part C, Emerging Technologies, Vol. 18, No. 6, 2010, pp. 963-974.

[15] I. Lymperopoulos and J. Lygeros, "Improved Multi-Aircraft Ground Trajectory Prediction for Air Traffic Control," Journal of Guidance, Control, and Dynamics, Vol. 33, No. 2, 2010, pp. 347–362.

[16] M. Margellos and J. Lygeros, "Toward 4-D Trajectory Management in Air Traffic Control: a Study Based on Monte Carlo Simulation and Reachability Analysis," IEEE Transanctions of Control System Technology, Vol. 21, No. 5, 2013, pp. 1820–1833.

[17] L.A. Weitz, "Investigating String Stability of a Time-History Control Law for Interval Management," Transportation Research Part C, Emerging Technologies, Vol. 33, 2013, pp. 257–271.

[18] G. Chaloulos, and J. Lygeros, "Effect of Wind Correlation on Aircraft Conflict Probability," Journal of Guidance, Control, and Dynamics, Vol. 30, No. 6, 2007, pp. 1742–1752.

[19] J. Hu, M. Prandini and S. Sastry, "Aircraft conflict prediction in the presence of a spatially correlated wind field," IEEE Transactions on Intelligent Transportation Systems, Vol. 6, No. 3, 2005, pp.326-340.

[20] Y. Matsuno, T. Tsuchiya, J. Wei, I. Hwang and N. Matayoshi, "Stochastic Optimal Control for Aircraft Conflict Resolution under Wind Uncertainty," Aerospace Science and Technology, Vol, 43, 2015, pp. 77-88.

[21] Q.M. Zheng and Y.J. Zhao, "Modeling Wind Uncertainties for Stochastic Trajectory Synthesis," AIAA Aviation Technology, Integration, and Operations Conference, Virginia Beach, VA, Sep. 20 - 22, 2011

[22] E. Hernandez, A. Valenzuela and D. Rivas, "Probabilistic Aircraft Conflict Detection Considering Ensemble Weather Forecast," 6th SESAR Innovation Days, the Netherlands, Nov. 8-10, 2016.

[23] D. Rivas, R. Vazquez and A. Franco, "Probabilistic Analysis of Aircraft Fuel Consumption using Ensemble Weather Forecasts," 7th International

Conference on Research in Air Transportation, Philadelphia, USA, Jun. 20-24, 2016.

[24] A. Motodani and N. Takeichi, "Prediction of Flight Time Uncertainty for 4D Trajectory Management," ENRI International Workshop on ATM/CNS, Tokyo, Japan, Nov. 14-16, 2017.

[25] N. Takeichi, and A. Motodani, "Feasibility Study on Modeling of Cruise Flight Time Uncertainty," 36th IEEE/AIAA Digital Avionics Systems Conference, St. Petersburg, FL, USA, Sep. 17-21, 2017.

[26] N. Takeichi, "Adaptive prediction of flight time uncertainty for ground-based 4D trajectory management," Transportation Research Part C, Emerging Technologies, Vol. 95, 2018, pp. 335–345.

[27] N. Takeichi, "An Adaptive Model of Flight Time Uncertainty and Its Application to Time-Based Air Traffic Operations," AIAA 2018-0423, AIAA Modeling and Simulation Technologies Conference, Kissimmee, Florida, Jan. 8–12, 2018.

[28] L.H. Mutuel, P. Neri and E. Paricaud, "Initial 4D Trajectory Management Concept Evaluation," 10th USA/Europe Air Traffic Management Research and Development Seminar, Chicago, Jun. 10-13,2013.

AUTHOR BIOGRAPHIES

Noboru Takeichi is a Professor of Department of Aeronautics and Astronautics at Tokyo Metropolitan University. He received B.E., M.E. and Ph.D in Engineering from The University of Tokyo in 1997, 1999 and 2002, respectively. After working for Japan Aerospace Exploration Agency and Electronic Navagation Research Institute as a researcher, he joined Department of Aerospace Engineering at Nagoya University as an associate professor in 2008, and moved to Tokyo Metropolitan University in 2015. His research interests include air traffic management and the future space systems, such as tethered systems, orbital elevator, etc. His e-mail address is takeichi@tmu.ac.jp.

Taiki Yamada is a graduate scholl student of Department of Aeronautics and Astronautics at Tokyo Metropolitan University. He received B.E. in Engineering from Tokyo Metropolitan University in 2018.

[29] A. Senoguchi and T. Koga, "Analysis of Downlink Aircraft Parameters Monitored by SSR Mode S in ENRI," 28th Digital Avionics Systems Conference, Orlando, Florida, Oct. 25-29, 2009.

[30] Japan Meteorological Agency, "High-Resolution GSM Data Service," http://www.wis-jma.go.jp/cms/gsm/ (cited Jan. 25, 2019)

[31] H.J. Berendsen, "A student's guide to data and error analysis," Cambridge University Press, 2011.

[32] T. Hastie, R. Tibshirani and J. Friedman, "The Elements of Statistical Learning: Data Mining, Inference, and Prediction, Second Edition," Springer, 2009.

[33] G. Schwarz, "Estimating the dimension of a model," The annals of statistics, Vol. 6, No. 2, 1978, pp.461-464.